Molecular Biology of the Cell
Vol. 17, 1697–1710, April 2006

Differential Requirements for Actin Polymerization, Calmodulin, and Ca^{2+} Define Distinct Stages of Lysosome/Phagosome Targeting

Walter Stockinger, Shao C. Zhang, Vishal Trivedi, Larissa A. Jarzylo, Eugenie C. Shieh, William S. Lane, Adam B. Castoreno, and Axel Nohturfft

Department of Molecular and Cellular Biology, The Biological Laboratories, Harvard University, Cambridge, MA 02138

Submitted December 18, 2005; Revised January 20, 2006; Accepted January 23, 2006
Monitoring Editor: Randy Schekman

Fusion of phagosomes with late endocytic organelles is essential for cellular digestion of microbial pathogens, senescent cells, apoptotic bodies, and retinal outer segment fragments. To further elucidate the biochemistry of the targeting process, we developed a scintillation proximity assay to study the stepwise association of lysosomes and phagosomes in vitro. Incubation of tritium-labeled lysosomes with phagosomes containing scintillant latex beads led to light emission in a reaction requiring cytosol, ATP, and low Ca^{2+} concentrations. The nascent complex was sensitive to disruption by alkaline carbonate, indicating that the organelles had "docked" but not fused. Through inhibitor studies and fluorescence microscopy we show that docking is preceded by a tethering step that requires actin polymerization and calmodulin. In the docked state ongoing actin polymerization and calmodulin are no longer necessary. The tethering/docking activity was purified to near homogeneity from rat liver cytosol. Major proteins in the active fractions included actin, calmodulin and IQGAP2. IQGAPs are known to bind calmodulin and cross-link F-actin, suggesting a key coordinating role during lysosome/phagosome attachment. The current results support the conclusion that lysosome/phagosome interactions proceed through distinct stages and provide a useful new approach for further experimental dissection.

INTRODUCTION

Phagocytosis is a multistep process involving binding of particles to cell surface receptors, formation of endocytic vesicles termed phagosomes, maturation of phagosomes to phagolysosomes, and finally digestion within phagolysosomes through the action of acidic hydrolases (Tartakoff *et al.*, 1999).

All stages of phagolysosome formation involve dynamic interactions with vesicles of the endosomal system. During particle engulfment, endosomes fuse with the phagosomal cup, providing membranes required for particle envelopment (Tapper and Grinstein, 1997; Bajno *et al.*, 2000; Braun *et al.*, 2004). At later stages, early endosomes, late endosomes, and lysosomes sequentially fuse with phagosomes to deliver proteins needed for degradation of luminal material (Desjardins *et al.*, 1994).

Colocalization of phagosomes and lysosomal markers has often been used as an end point of phagosome maturation, and many proteins have been identified that are required for completion of this process (Vieira *et al.*, 2002). Actin, in particular, has emerged as a key factor at several stages along the phagocytic pathway. Signaling downstream from phagocytic receptors results in actin polymerization, which leads to plasma membrane extrusion and the eventual engulfment of the particle (Castellano *et al.*, 2001; May and Machesky, 2001). Often, newly formed phagosomes then translocate to the perinuclear region in a process that may involve both microfilaments and microtubules (Toyohara and Inaba, 1989; Blocker *et al.*, 1998; Moller *et al.*, 2000). Finally, F-actin formation on the surface of late endosomes, lysosomes and phagosomes has been shown to be required for eventual fusion (Jahraus *et al.*, 2001). Actin polymerization on these membranes requires phosphorylation of phosphatidylinositol and recruitment of two ERM domain proteins, ezrin, and/or moesin, that have the ability to both bind membranes and nucleate F-actin (Defacque *et al.*, 2000, 2002).

To further elucidate the biochemical processes that lead to fusion we have developed a scintillation proximity assay to study lysosome/phagosome interactions in vitro. The approach allowed us to distinguish three phases. In phase 1 lysosomes and phagosomes attach in a reaction requiring ATP, actin polymerization, calmodulin, other cytosolic factors, and an absence of Ca^{2+}. During phase 2 a complex forms that is characterized by being insensitive to inhibitors of calmodulin and actin polymerization but sensitive to alkaline carbonate, which disrupts protein/protein interactions. In phase 3 exposure of the docked organelles to Ca^{2+} causes further consolidation of the complex as indicated by resistance to disruption by alkaline carbonate.

This article was published online ahead of print in *MBC in Press* (http://www.molbiolcell.org/cgi/doi/10.1091/mbc.E05–12–1140) on February 1, 2006.

Address correspondence to: Axel Nohturfft (axno@mcb.harvard.edu).

Abbreviations used: PVT, polyvinyltoluene.

MATERIALS AND METHODS

Reagents

We obtained egg yolk phosphatidylcholine (P-2772), dioleoyl phosphatidylserine, dicetyl phosphate, protease inhibitor cocktail, 4-methylumbelliferyl alpha-D-mannopyranoside, 4-methylumbelliferyl *N*-acetyl-β-D-glucosaminide dihydrate, mouse IgG, trifluoperazine, latrunculin A, cytochalasin B, monoclonal actin antibody (AC-40), and purified calmodulin (P0809) from

Sigma (St. Louis, MO); purified actin from Cytoskeleton, Inc. (APHL95, Denver, CO); W5, W7, and calmidazolium from Calbiochem (La Jolla, CA); [1,2-^{3}H]cholesterol from Perkin Elmer; [1,2-^{3}H]cholesteryl oleate, [1,2-^{3}H]cholesteryl oleoyl ether, scintillant yttrium silicate (YSi) beads, and polyethyleneimine-coated scintillant polyvinyltoluene (PVT) beads from GE Healthcare (Uppsala, Sweden); pepstatin A, GTP, ATP, creatine kinase, and creatine phosphate from Roche; leupeptin from Peptide Institute (Osaka, Japan); horseradish peroxidase–conjugated anti-mouse and anti-rabbit IgG from Jackson ImmunoResearch Laboratories (West Grove, PA); amine-coated latex beads from Bangs Laboratories (Fishers, IN); polyclonal antibody against calmodulin from Zymed (61–8500; South San Francisco, CA); polyclonal antibody against Cdc42/Rac1 from Chemicon (AB3302, Temecula, CA); monoclonal antibody against IQGAP2 from Upstate Biotechnology (clone BB9; Lake Placid, NY); fetal bovine serum (FBS) from Invitrogen (Carlsbad, CA) and other cell culture reagents from Mediatech (Herndon, VA). Anionic liposomes were prepared as described (Aikawa *et al.*, 1994) and contained 1 mM phosphatidylcholine, 1 mM phosphatidylserine, 0.2 mM dicetyl phosphate, and 200 μCi/ml radiolabeled lipids as indicated below.

Buffers

ATP-regenerating system was prepared as an 8× stock solution containing 8 mM ATP, 2 mM GTP, 40 mM creatine phosphate, and 0.02 mg/ml creatine kinase. The pH was adjusted to 7.3 with KOH. Buffer A corresponds to 10 mM HEPES (pH 7.0), 10 mM KCl, 1.5 mM $MgCl_2$, 1 mM DTT, and protease inhibitors (1 μg/ml pepstatin A plus 5 μg/ml leupeptin). Buffer B corresponds to 40 mM HEPES (pH 7.0), 250 mM sucrose, 100 mM KCl, 3 mM $MgCl_2$, and 0.5 mM EGTA plus protease inhibitors. Buffer C corresponds to 40 mM HEPES (pH 7.3), 250 mM sucrose, 0.7 M ammonium sulfate, 100 mM KCl, 3 mM $MgCl_2$, and 0.5 mM EGTA plus protease inhibitors. Buffer D corresponds to 40 mM HEPES (pH 7.3), 250 mM sucrose, 50 mM KCl, 3 mM $MgCl_2$, and 0.5 mM EGTA plus protease inhibitors. Buffer E corresponds to 40 mM HEPES (pH 7.3), 250 mM sucrose, 500 mM KCl, 3 mM $MgCl_2$, and 0.5 mM EGTA plus protease inhibitors. Buffer F corresponds to buffer B plus 30% sucrose. Buffer G corresponds to 40 mM HEPES (pH 7.3), 3 mM $MgCl_2$, and 0.5 mM EGTA plus 100 mM KCl.

Preparation of Rat Liver Cytosol

Male CD rats were killed by CO_2 inhalation, and the liver was perfused with phosphate-buffered saline (PBS) through the portal vein until the color changed to pale pink. Livers were excised, rinsed three times with ice-cold PBS, cut into small pieces, rinsed again three times with PBS and transferred to a 50-ml tube containing 13 ml ice-cold buffer B. All subsequent steps were performed on ice or at 4°C. The tissue was homogenized using a Polytron homogenizer for 10 s at maximum speed and centrifuged at 3600 × *g* for 30 min in a Sorvall Legend RT centrifuge (Newton, CT). The resulting supernatant was centrifuged again for 45 min at 270,000 × *g* in a Beckman L8–70 ultracentrifuge (Fullerton, CA) equipped with an SW40T rotor and again for 4 h at 270,000 × *g*. After each ultracentrifugation step, the white top layer was removed and the remaining supernatant was transferred to new centrifuge tubes. Aliquots were snap-frozen in liquid nitrogen and stored at −80°C.

Protein Analyses

Protein was quantified by the Lowry method or with Coomassie Plus Reagent (Pierce, Rockford, IL) using bovine serum albumin as a standard. Western blots were developed with Super Signal Enhanced Luminescence Solution (Pierce).

Cell Culture

J774 mouse macrophages were grown in monolayer culture at 37°C in an atmosphere of 8–9% CO_2 in medium A (a 1:1 mixture of Ham's F-12 medium and DMEM plus 100 U/ml penicillin, 100 μg/ml streptomycin sulfate plus 10% [vol/vol] FBS). Medium B is identical to medium A but lacks phenol red.

Preparation of Postnuclear Supernatants

On day 0, J774 cells were set up in 10-cm dishes at 70–90% confluency in 4 ml of medium A supplemented either with liposomes containing [^{3}H]cholesteryl oleoyl ether (16 μCi/dish/4 ml medium) or with 0.01 mg/ml Alexa Fluor 594 hydrazide (Invitrogen). After incubation at 37°C for 16 h, cells were washed three times with PBS, once with buffer A, and scraped into 1 ml of buffer A. Cell suspensions were passed five times through a bent 22-gauge needle and centrifuged at 1000 × *g* for 5 min. Postnuclear supernatants were prepared fresh for each experiment.

Gradient Centrifugation

Protocol 1: 30% Percoll gradient centrifugation as described (Lange *et al.*, 1998). Samples were divided into 13 1-ml fractions. Radioactivity peaked in fraction 3, which contained 25% of β-hexosaminidase activity, 15% of α-mannosidase II activity, 76% of NADPH-cytochrome c reductase activity, 26% of 5′nucleotidase activity, and 64% of radioactivity. Protocol 2: The sucrose concentration of postnuclear supernatants was adjusted to 60% (wt/vol). The solution was overlaid with a linear 50–15% sucrose gradient and centrifuged at 40,000 rpm for 16 h in a SW40T rotor. Protocol 3: 2 10-cm dishes of J774 cells were labeled with [^{3}H]cholesteryl ether, and a postnuclear supernatant was prepared as described above. Sucrose was added to a final concentration of 50%. The mixture was overlaid with a 50–10% linear sucrose gradient in buffer B and centrifuged at 40,000 rpm for 210 min in an SW40T rotor.

The activities of Golgi α-mannosidase II, lysosomal β-hexosaminidase (Storrie and Madden, 1990), endoplasmic reticulum NADPH-cytochrome c reductase (Sillence and Downes, 1993), plasma membrane 5′nucleotidase (Liscum *et al.*, 1989), and tritium were determined as described in the indicated references.

Isolation of Phagosomes

J774 cells were set up in 10-cm dishes at 70–90% confluency. On day 1 of growth, each dish received a suspension of 20 mg of polyethyleneimine-coated scintillant PVT beads in 1 ml medium A. After 60 min the medium was removed, cells were washed with PBS, refed with prewarmed medium A and incubated for another 60 min. Cells were then washed three times with PBS, once with buffer F, and scraped into 1 ml buffer F. All subsequent steps were performed on ice or at 4°C. Cell suspensions were overlaid with 12 ml of a linear 30–0% sucrose gradient in buffer B and centrifuged at 270,000 × *g* for 30 min in an SW40T rotor. The phagosomes focused in a narrow visible band and were collected in a volume of 1.5 ml. Phagosomes separate from cells during centrifugation and no homogenization step was found to be necessary. Bead concentrations were estimated by measuring the OD600 using suspensions with known concentrations of PVT beads for calibration. Phagosome fractions prepared by this method are enriched for lysosomal markers and contain little cytosolic or plasma membrane markers (Stockinger *et al.*, 2004). Phagosomes were prepared fresh for each experiment.

Cell-free Scintillation Proximity Assay

Reactions were set up in 1.5-ml microcentrifuge tubes and contained 0.75 mg phagosomes (added in a volume of ~50 μl), postnuclear supernatant from [^{3}H]cholesteryl oleoyl ether labeled J774 cells (containing ~80 μg protein and ~40 nCi tritium; added in a volume of ~50 μl), 50 μl of an 8× ATP-regenerating system, and 6 mg/ml rat liver cytosol (added in a volume of ~50 μl). Reactions were brought to a final volume of 400 μl by addition of buffer B plus 250 mM sucrose, rotated at 37°C for the indicated time, and placed on ice for 3 min. To determine proximity scintillation, tubes were inserted into 20-ml glass scintillation vials and analyzed in a Beckman LS 6000 IC scintillation counter. Where indicated, samples were subsequently supplemented with sodium carbonate (pH 11, 0.1 M final concentration) and vortexed at maximum speed for 10 s. Proximity scintillation was then measured again as above.

Protein Identification by Tandem Mass Spectrometry

Coomassie stained and excised SDS-PAGE bands were subjected to in gel reduction, carboxyamidomethylation, and digestion with trypsin. Peptide sequences were determined using a 75-μm reverse-phase microcolumn terminating in a custom nanoelectrospray source (New Objective) directly coupled to an LCQ DECA XP Plus linear quadrupole ion trap mass spectrometer (Thermo Electron, Pittsburgh, PA). The instrument was operated in data-dependent mode fragmenting (relative collision energy = 30%, isolation width = 2.5 Da, dynamic exclusion) on the four most abundant ions in each survey scan. Preliminary sequencing of peptides was facilitated by NCBI nr database correlation with the algorithm SEQUEST, and an in-house spectrum review workbench, FuzzyIons. All spectra were manually inspected for completeness of ion assignments and intensity-based signatures (e.g., neutral loss(es), proline ions, etc.).

Actin Labeling

Human nonmuscle actin (1 mg; Cytoskeleton, Inc.) was labeled with 1 mg fluorescein isothiocyanate (FITC, Sigma) in 100 μl of 0.1 M sodium bicarbonate buffer (pH 9) at room temperature for 1 h. The reaction product was separated from unincorporated dye by purification on a NAP-10 Sephadex-G25 column (GE Healthcare).

Analysis of In Vitro Reaction Products by Confocal Microscopy

Cell-free reactions were performed as described above except that postnuclear supernatants were prepared from J774 cells grown with Alexa Fluor 594 hydrazide as a lysosomal fluid-phase marker. Reactions were terminated by transfer on ice for 3 min. Phagosomes were pelleted by centrifugation at 1000 × *g* for 5 min, washed once in buffer B, and mounted on glass slides in Fluoromount G (Southern Biotechnology, Birmingham, AL). Actin was visualized either by including 0.1 mg/ml FITC-labeled actin during in vitro incubations or by staining pelleted reaction products with 50 μg/ml FITC-phalloidin (Sigma) for 30 min.

For calmodulin staining reaction products were blocked for 1 h with 2% BSA in PBS after fixation and then incubated for 1 h with 2.5 μg/ml poly-

clonal calmodulin antibody (Zymed). Detection of the antibody was performed using a tyramide signal amplification system (TSA Kit 12, Invitrogen) consisting of HRP-goat anti-rabbit IgG and Alexa Fluor 488 tyramide according to the manufacturer's protocol.

Microscopy was performed on a Zeiss Axiovert 100 microscope equipped with a Zeiss LSM510 META confocal system (Thornwood, NY). Excitation wavelengths for scintillant PVT beads, FITC-actin, and Alexa 594 hydrazide were 364, 488, and 543 nm, respectively. Pictures were taken with a 64× objective in multitrack mode. The pinhole was adjusted to yield a 3-μm optical slice.

RESULTS

Cell-free Phagosome/Lysosome Docking Assay

Phagosome/lysosome interactions were studied with a cell-free scintillation proximity assay consisting of tritium-labeled donor membranes, phagosome acceptors containing scintillant latex beads, cytosol, and nucleoside triphosphates. In this assay light emission results when β particles are absorbed by scintillant beads. Because of the short range of tritium-derived β radiation and because of geometric constraints, scintillation can only be elicited by labeled vesicles that are in close vicinity (within ~600 nm) of the scintillant (Hart and Greenwald, 1979; Stockinger *et al.*, 2004).

Acceptors containing scintillant beads were isolated by sucrose gradient centrifugation from J774 mouse macrophages after 1 h of phagocytosis followed by a 1-h chase. The strategy for labeling donor vesicles is based on the definition of lysosomes as the terminal degradative compartment of the endocytic pathway and, as such, as the depository of indigestible material (de Duve, 1963; Scriver *et al.*, 2001). As a lysosomal tracer we chose tritiated cholesteryl oleoyl ether ("[^{3}H]cholesteryl ether"), a nonhydrolyzable analog of cholesteryl fatty acyl esters (Stein *et al.*, 1980) that can efficiently be fed to macrophages as a component of liposomes. In J774 cells, <1% of [^{3}H]cholesteryl ether was hydrolyzed after 16 h of incubation (unpublished data).

When donor and acceptor membranes are mixed and incubated in vitro, scintillation is produced in a temperature-, ATP- and cytosol-dependent manner (Figure 1A). The signal remained low when naked beads were used instead of phagosomes (Figure 1A) or when donor or acceptor membranes were pretreated with protease (unpublished data), indicating that the interaction between donors and acceptors requires intact membranes. ATP was routinely added together with an ATP-regenerating system and GTP. However, omission of GTP from the reaction had no negative effect (unpublished data).

To verify that lysosomes serve as the primary donor during the assay, we performed a series of experiments that are shown in Figure 1 B–D. First, J774 cells were labeled with [^{3}H]cholesteryl ether overnight and fractionated by sucrose gradient centrifugation. Individual fractions were then combined with phagosomes, cytosol, and triphosphonucleosides and analyzed in vitro as above. Proximity scintillation, lysosomal β-hexosaminidase activity, and total radioactivity all peaked in the same fraction (Figure 1B).

To analyze the subcellular distribution of [^{3}H]cholesteryl ether in more detail, cells were labeled as above and then subjected to sequential Percoll and sucrose gradient centrifugation. After the second centrifugation step, fractions were analyzed for radioactivity and enzyme markers characteristic of lysosomes, ER, Golgi, and plasma membrane. As shown in Figure 1C, the radioactivity profile closely matched that of lysosomes. These results are consistent with previous studies on macrophages demonstrating that inert components of liposomes are endocytosed and transported to lysosomes (Daleke *et al.*, 1990; Yoshimura *et al.*, 1995).

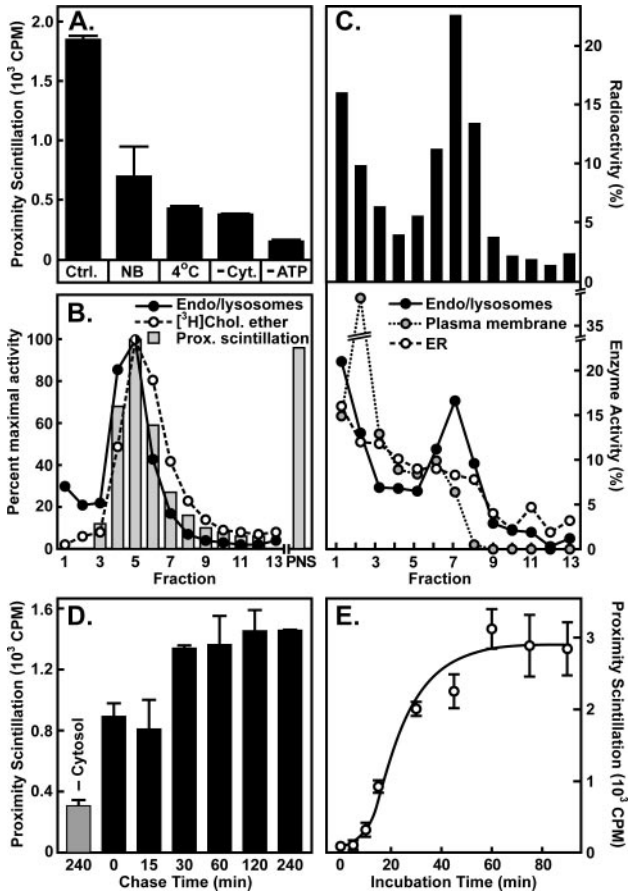

Figure 1. In vitro assay for phagosome/lysosome docking. (A) Postnuclear supernatants (PNS, "donors") were prepared from J774 cells incubated for 16 h with liposomes containing [^{3}H]cholesteryl oleoyl ether (see *Materials and Methods*). Phagosomes containing scintillant PVT beads ("acceptors") were prepared as described in *Materials and Methods*. Donors and acceptors were mixed with rat liver cytosol and an ATP-regenerating system. Samples were incubated at 37°C for 1 h. Negative control reactions were performed with naked beads instead of phagosomes (NB), on ice (4°C), in the absence of rat liver cytosol (-Cyt.), and in the absence of an ATP-regenerating system (-ATP). Proximity scintillation was measured in a scintillation counter. (B) A PNS was prepared from one 10-cm dish of J774 macrophages that had been grown for 16 h in the presence of liposomes containing [^{3}H]cholesteryl oleoyl ether and then fractionated by sucrose gradient centrifugation as described in *Materials and Methods* (Protocol 3). Fractions were analyzed for β-hexosaminidase activity (Endo/lysosomes), radioactivity ([^{3}H]Chol. ether), and their ability to serve as donors in the scintillation proximity assay. In vitro reactions were set up as in A except that PNSs were replaced with 120 μl of the indicated gradient fraction plus 80 μg of J774 cell cytosol. One sample with PNS was included as a positive control. (C) J774 cells were loaded with [^{3}H]cholesteryl ether as in B. The sample was then subjected to Percoll gradient centrifugation (*Materials and Methods*, Protocol 1). Fraction 3 was further fractionated by sucrose gradient centrifugation (*Materials and Methods*, Protocol 2). Fractions were collected from the bottom of the tube and analyzed for total radioactivity (top panel) and organellar markers (bottom panel). (D) Reactions were performed as in A except that PNSs were prepared from cells that had been subjected to a pulse-chase protocol: confluent J774 cells in 6-cm dishes were incubated with liposomes containing [^{3}H]cholesteryl ether (12.5 μCi/dish/ml medium) for 4 h at 15°C. The cells were then washed, refed with medium A, and incubated at 37°C for the indicated time. Reactions were set up with PNS aliquots containing equal amounts of radioactivity. (E) Reactions were set up as in A and incubated at 37°C for the indicated time. Error bars, SD (n = 2).

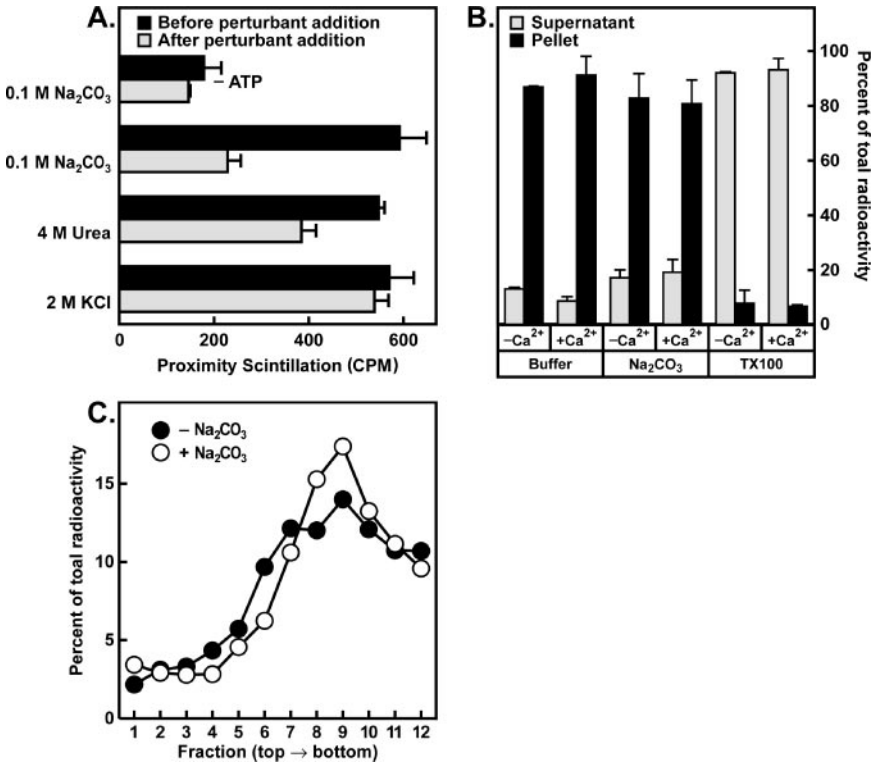

Figure 2. Stability of lysosome/phagosome complexes. (A) In vitro reactions were set up as in Figure 1A and incubated at 37°C for 1 h. Proximity scintillation was determined in a scintillation counter (black bars). Reactions were then supplemented with 0.1 M sodium carbonate (pH 11), 4 M urea, or 2 M KCl (final concentrations) and vortexed for 10 s, and scintillation was immediately measured again (gray bars). (B) On day 0, J774 cells were set up at 50% confluency in a 6-cm dish and incubated with liposomes containing [^{3}H]cholesteryl oleoyl ether. On day 1, a postnuclear supernatant was prepared and aliquots were mixed with rat liver cytosol and ATP-regenerating system as in Figure 1A but without phagosomes. Reactions were incubated in the absence or presence of 1 mM Ca^{2+} at 37°C for 1 h. Subsequently, samples were supplemented with buffer, Na_2CO_3, (pH 11, 0.1 M final concentration) or Triton X-100 (1% final concentration) as indicated, vortexed for 10 s, and centrifuged at 16,000 × *g* for 30 min at 4°C. Radioactivity was determined in supernatant and pellet. Data represent radioactivity in individual fractions divided by the total radioactivity in supernatant plus pellet. Error bars, SD (n = 3). (C) Postnuclear supernatants were prepared from a 10-cm dish of J774 cells loaded with [^{3}H]cholesteryl ether and from a 10-cm dish of unlabeled cells. The samples were mixed, split into equal aliquots, supplemented with buffer or Na_2CO_3, and overlaid with a linear sucrose gradient (50–15%). Samples were centrifuged at 270,000 × *g* for 3 h. One-milliliter fractions were collected from the top and analyzed for total radioactivity.

In the course of maturation phagosomes exchange material with vesicles from all compartments of the endosomal system (Pitt *et al.*, 1992; Desjardins *et al.*, 1994). To compare the ability of early endosomes, late endosomes and lysosomes to interact with phagosomes in vitro, we performed the experiment shown in Figure 1D. First, macrophages were loaded with [^{3}H]cholesteryl ether-containing liposomes at 15°C to label early endosomes (Brown and Goldstein, 1976; Dunn *et al.*, 1980; Sullivan *et al.*, 1987). Subsequently, the cells were washed and shifted to 37°C for different periods to allow movement of the tracer to later compartments of the endosomal system (Steinman *et al.*, 1976; Storrie *et al.*, 1984). When postnuclear supernatants from these cells were analyzed in the cell-free assay, we found that extracts from all time points produced a scintillation signal well above background (Figure 1D). However, the signal increased by 65% between 15 and 30 min ($p < 0.035$) and then remained stable up to 4 h of chase. The observed transition phase corresponds to the time expected for transport from early to late endosomes (Wolkoff *et al.*, 1984; Wall and Hubbard, 1985; Dunn *et al.*, 1986), suggesting that the conditions of the cell-free assay favor phagosome interactions with late endosomes and lysosomes. In all subsequent experiments donor membranes were prepared from cells loaded with [^{3}H]cholesteryl ether at 37°C overnight as in Figure 1, A–C.

In Figure 1E, in vitro reactions were incubated for different periods of time. The scintillation signal began to increase with a delay of ~15 min, suggesting that lysosomes and phagosomes interact in a multistep process.

To determine how tightly lysosomes and phagosomes interact during the in vitro reaction, samples were incubated at 37°C for 1 h, and scintillation was measured before and after treatment with reagents that disrupt protein–protein and protein–membrane interactions. The signal was resistant to 2 M salt and only partially sensitive to 4 M urea, demonstrating that interactions are very stable (Figure 2A; Gilmore and Blobel, 1985). However, after treatment with 0.1 M sodium carbonate at pH 11, the signal returned to background levels. Inasmuch as alkaline carbonate disrupts protein–protein and protein-membrane interactions but does not dissolve bilayers (Fujiki *et al.*, 1982), these results suggest that lysosomes and phagosomes are only reversibly attached.

To control for the possibility that alkaline carbonate might have reduced the scintillation signal by causing the release of [^{3}H]cholesteryl ether from vesicles, we performed the experiments in Figure 2, B and C. First, postnuclear supernatants from [^{3}H]cholesteryl ether–loaded cells were incubated for 1 h with ATP and cytosol at 37°C. The samples were then supplemented with sodium carbonate and centrifuged, and radioactivity was measured in supernatants and pellets. Compared with buffer-treated controls, no significant changes were seen after carbonate treatment (Figure 2B). Although these results indicate that cholesteryl ether remained membrane-bound, as would have been expected from its hydrophobicity, they do not rule out that cholesteryl ether might have leaked from lysosomes or phagolysosomes and partitioned into other vesicles. To address this possibility, postnuclear supernatants from [^{3}H]cholesteryl ether–loaded cells were combined with an equal amount of postnuclear supernatant from unlabeled cells. Mixtures were then supplemented with buffer or alkaline carbonate and fractionated by density gradient centrifugation. If alkaline carbonate had caused a redistribution of [^{3}H]cholesteryl ether, one would have expected a broadening of the radioactivity profile, but this was not observed (Figure 2C). Collectively, the results in Figure 2 indicate that the in vitro reaction arrests at a stage

where lysosomes and phagosomes have "docked" but not fused.

Ca^{2+} Confers Carbonate Resistance to the Lysosome/Phagosome Complex

Although the above-described in vitro reactions were performed in the absence of Ca^{2+}, several studies have come to the conclusion that elevated Ca^{2+} concentrations correlate with fusion of lysosomes and phagosomes in intact cells (Jaconi *et al.*, 1990; Malik *et al.*, 2000). However, the literature on the issue is divided (Zimmerli *et al.*, 1996; Myers and Swanson, 2002). The Ca^{2+} concentration in cytosol is usually around 100 nM but can transiently increase to micromolar levels in response to extracellular stimuli. Binding of IgG-opsonized particles to Fc receptors has been shown to trigger trains of Ca^{2+} spikes that can propagate as waves across the cell (Jaconi *et al.*, 1990; Myers and Swanson, 2002; Worth *et al.*, 2003).

Addition of Ca^{2+} to the in vitro reaction at concentrations up to 100 nM had no effect (unpublished data). However, at higher concentrations, Ca^{2+} was inhibitory and at 2 mM docking was reduced by 92% (Figure 3A, reaction b). Because cellular Ca^{2+} spikes are usually rare and brief, it is plausible that initial contact formation between lysosomes and phagosomes proceeds optimally when Ca^{2+} concentrations are low. We thus hypothesized that Ca^{2+} might act specifically on those lysosome/phagosome complexes that have already formed a docked configuration. In fact, when docking is allowed to proceed in the absence of Ca^{2+} for 1 h, and Ca^{2+} is then added for another hour, the scintillation signal remains high (Figure 3A, reaction c).

To further examine the effect of Ca^{2+} on docked lysosome/phagosome complexes, we then measured the sensitivity of the scintillation signal to alkaline carbonate. Cell-free reactions were again performed in two steps: first, in the absence of Ca^{2+} for 1 h and then minus or plus 2 mM Ca^{2+} for an additional hour. When measured immediately thereafter, the scintillation signal was equally high in samples with or without Ca^{2+} (Figure 3B, reactions a and b; black bars) and this effect was dependent on cytosol and ATP (reactions c and d). However, after carbonate treatment the outcome was significantly different: In the absence of Ca^{2+} scintillation dropped by 79%, whereas in the presence of Ca^{2+} the signal remained high (reactions a and b, gray bars). These results indicate that Ca^{2+} acts on docked lysosome/phagosome complexes by triggering the formation of a carbonate-resistant complex.

The time dependence of Ca^{2+} action was determined by incubating reactions in the absence of Ca^{2+} for 1 h and then in the presence of Ca^{2+} for different periods. As shown in Figure 3C, maximal carbonate resistance requires ~1 h of incubation with Ca^{2+}. The free Ca^{2+} concentration required for half-maximal carbonate resistance lies between 1 and 10 μM (Figure 3D).

Fluorescence Microscopy of Lysosome/Phagosome Interactions In Vivo

The data in Figures 1–3 support a model in which lysosome/phagosome targeting proceeds in at least two stages. During stage one the organelles reversibly attach under conditions requiring the presence of ATP, cytosolic factors and low Ca^{2+} concentrations; subsequent exposure of the docked complex to Ca^{2+} and then triggers a consolidation process that eventually leads to fusion. In search of support for this model in intact cells, we performed a series of fluorescence microscopy experiments. RAW 264.7 macrophages were exposed to latex beads for 7 min, washed to remove unincorporated beads, and chased for up to several hours. Subsequently, the cells were fixed and incubated with an antibody against the late endosomal/lysosomal membrane protein Lamp2 (Chen *et al.*, 1985). To distinguish between phagosomes and extracellular beads, the samples were also stained with filipin, a fluorescent antibiotic that stains cholesterol-containing membranes (Bornig and Geyer, 1974). Analysis of samples from multiple experiments led us to distinguish three classes of phagosomes. Type I phagosomes were positive by filipin staining but had little or no associated Lamp2 fluorescence. Type II phagosomes were surrounded by discontinuous Lamp2 staining that had the appearance of vesicles attached to the surface of the phagosome rather than Lamp2 being part of the phagosomal membrane itself. In phagosomes classified as type III, Lamp2 staining around the beads was visible as a smooth ring, suggesting that the protein had incorporated into the limiting phagosomal membrane. Representative images of phagosomes after 30 min of chase are shown in Figure 4. Examples of type II phagosomes are shown in the insets of

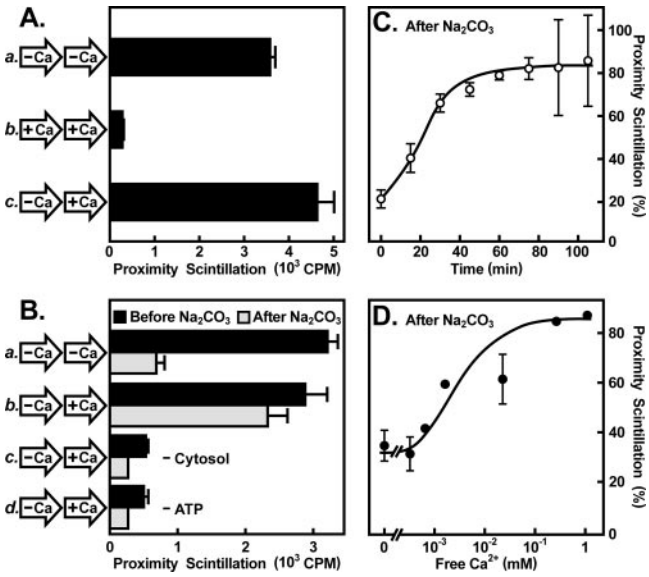

Figure 3. Ca^{2+}-induced consolidation of lysosome/phagosome complexes in vitro. (A) Docking reactions were set up as described in Figure 1A and all samples were incubated at 37°C for 2 h. In reactions b and c 2 mM $CaCl_2$ (final concentration) was present either throughout or only during the second half on the incubation period as indicated. (B) Reactions were set up in Ca^{2+}-free buffer and incubated at 37°C for 1 h. Control reactions were set up in the absence of rat liver cytosol and ATP as indicated. Subsequently, samples received buffer (reaction a) or buffer plus Ca^{2+} (2 mM final concentration; reactions b–d). Reactions were continued for 1 h at 37°C. Proximity scintillation was determined before (black bars) and after sodium carbonate treatment (gray bars) as in Figure 2. (C) Reactions were set up in Ca^{2+}-free buffer and incubated for 1 h at 37°C as above. Each sample then received Ca^{2+} to a final concentration of 2 mM and incubations were continued for the indicated time. Proximity scintillation was determined before and after sodium carbonate treatment. Data represent scintillation counts after sodium carbonate addition divided by the scintillation counts measured before sodium carbonate addition. (D) Reactions were set up in Ca^{2+}-free buffer and incubated for 1 h at 37°C as above. Samples then received buffer or Ca^{2+} at different concentrations and incubations were continued for 1 h at 37°C. Free Ca^{2+} concentrations were calculated using Winmax software (Patton *et al.*, 2004). Proximity scintillation was determined before and after sodium carbonate treatment. Data are plotted as in C. Error bars, SD (n = 2).

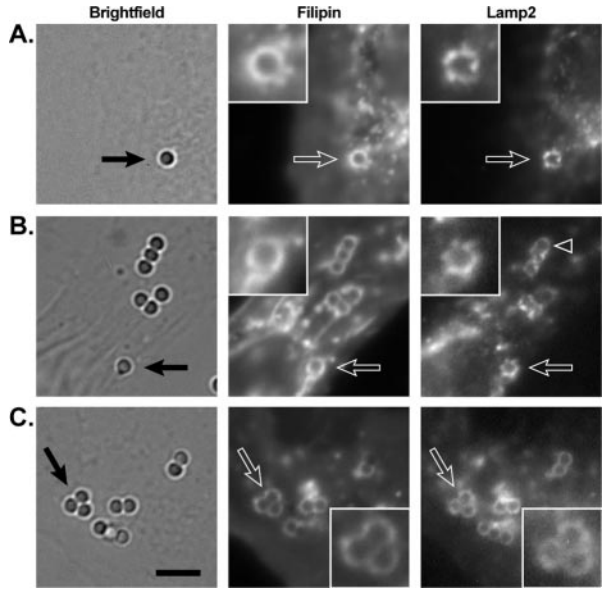

Figure 4. On day 0, RAW 264.7 macrophages were set up on cover slips in a 24-well plate in medium A. On day 1, cells received 10 μg/well of 0.75-μm latex beads. The plate was centrifuged for 2 min at 1000 $\times$ *g* and incubated at 37°C for 5 min. The cells were then washed three times with PBS and incubated for an additional 30 min at 37°C. Subsequently, cells were fixed with 4% paraformaldehyde, permeabilized with 0.1% Triton X-100 in PBS, blocked, incubated with anti Lamp2 antibody (ABL-93; 1:100; Developmental Studies Hybridoma Bank, Iowa City, IA) and then stained with secondary antibody conjugated to Alexa Fluor 546 (1:400; Invitrogen) plus 50 μg/ml filipin (Polysciences, Warrington, PA). The coverslips were washed three times with PBS and mounted in Fluoromount-G (Southern Biotechnology, Birmingham, AL). Slides were analyzed on a Nikon Eclipse TE300 inverted microscope (Melville, NY) equipped with a Nikon 100$\times$ objective and a Spot RT Monochrome camera. Arrows point at areas that are enlarged in the insets. The arrowhead points at a phagosome with mixed type II/III appearance. Bar, 3 μm.

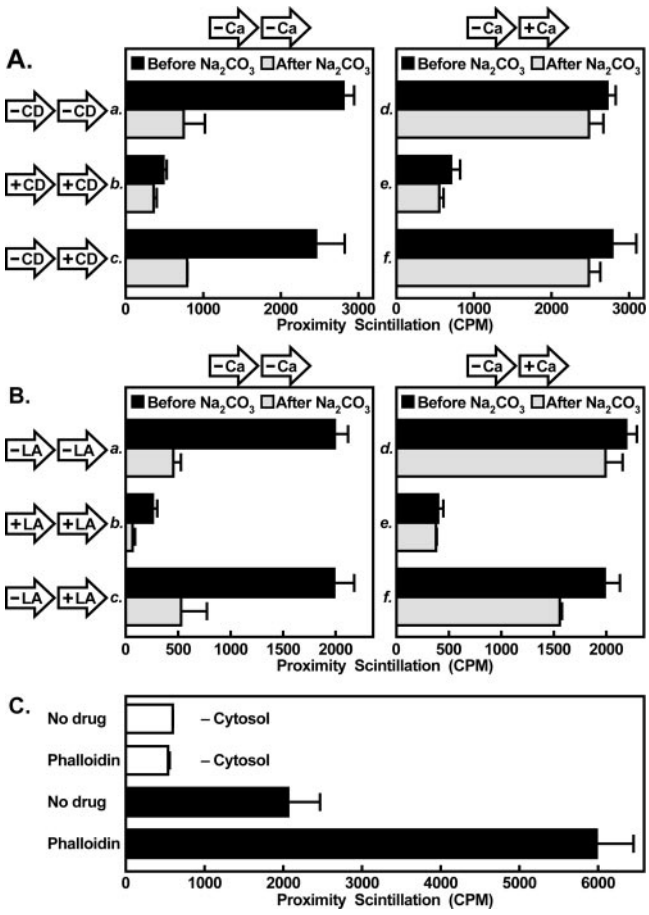

Figure 5. Actin polymerization is required for phagosome/lysosome docking in vitro. (A) Two-step docking reactions were performed as in Figure 3B. Left, all reactions were performed in the absence of Ca^{2+}; right,: 2 mM Ca^{2+} was added during phase 2. Cytochalasin D (20 μM; CD) was present during phase 1 and phase 2 or only during phase 2 as indicated. Proximity scintillation was determined before (black bars) and after (gray bars) sodium carbonate treatment as in Figure 2. (B) Reactions were performed as in A, except that 1 μM latrunculin A (LA) was used instead of cytochalasin D. (C) Cell-free docking reactions were performed for 1 h in the absence or presence of rat liver cytosol and 10 μM phalloidin as indicated. Error bars, SD (n = 2).

Figure 4, A and B, and several type III phagosomes can be seen in Figure 4C. In many cases, phagosomes appeared as a mixture of the two types, such as that marked by an arrowhead in Figure 4B. Type I phagosomes were observed only between 0 and 15 min of chase. Both type II, type III and mixed type II/III phagosomes were observed between 30 min and 2 h of chase. After 4 h only type III phagosomes could be observed (unpublished data). Similar results were obtained when lysosomes were labeled with fluorescent dextran and in cells expressing a Lamp1-RFP fusion protein (unpublished data). Collectively, these results support the conclusion that fusion of lysosomes with phagosomes is preceded by a "docking" stage.

Lysosome/Phagosome Attachment Requires Actin Polymerization

We next sought to identify some of the cytosolic factors that are required for the ATP-dependent attachment process. Previous studies have shown that proteins on the surface of late endosomes and phagosomes can induce the assembly of filamentous actin, leading to formation of endosome/endosome and endosome/phagosome aggregates in vitro (Defacque *et al.*, 2000; Kjeken *et al.*, 2004). Further, actin polymerization was shown to be required for endosome/phagosome fusion in vitro and in vivo (Jahraus *et al.*, 2001).

To determine at which step of the targeting process actin is required, cytochalasin D, an inhibitor of actin polymerization, was added at different stages of the cell-free scintillation proximity assay (Figure 5A). After 2 h of incubation in the absence of cytochalasin D and Ca^{2+}, a complex was formed that disassembled upon addition of carbonate (left panel, reaction a). When cytochalasin D was added at the beginning of the reaction, attachment was blocked (reaction b). When reactions were allowed to proceed to 1 h and cytochalasin D was added only during the second half of the reaction, docking was unaffected (reaction c).

To determine whether ongoing actin polymerization is also required subsequent to docking, some samples received Ca^{2+} during phase two of the reaction (Figure 5A, right panel). Under control conditions a complex formed that remained resistant to alkaline carbonate (reaction d). If cytochalasin D was present from the start, complex formation was blocked (reaction e). When cytochalasin D was added only during phase 2 together with Ca^{2+}, the drug was again without effect (reaction f). Similar results were obtained with another actin inhibitor, latrunculin A (Figure 5B).

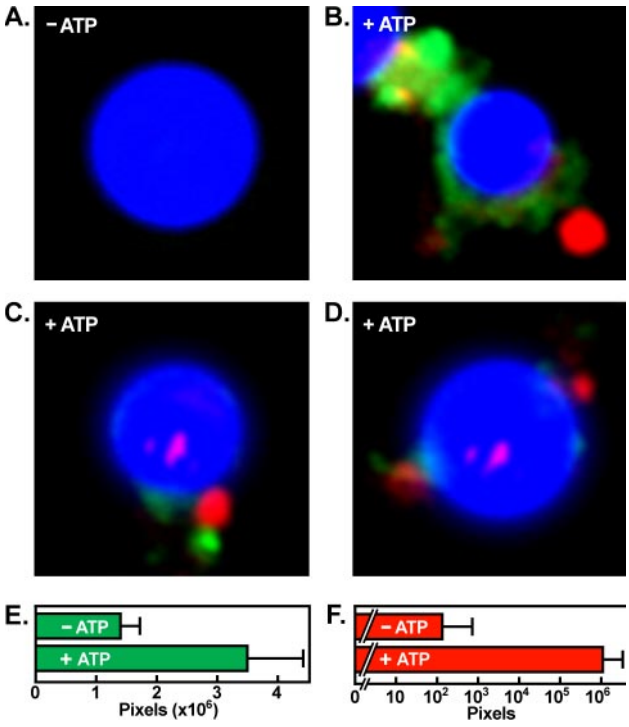

Figure 6. Analysis of in vitro reactions by fluorescence microscopy. (A–D) Reactions were performed as in Figure 1A, except that reactions were supplemented with FITC-actin and donor membranes were loaded with Alexa Fluor 594 hydrazide. Reactions were set up in the absence (A) and presence (B–D) of an ATP-regenerating system. Samples were then fixed and analyzed by confocal fluorescence microscopy. PVT beads are shown in blue, FITC-actin is green and Alexa Fluor 594 hydrazide is red. (E and F) Reactions were performed as above, except that that FITC-actin was omitted. Samples were then fixed, stained with FITC-phalloidin, and analyzed by confocal fluorescence microscopy. (E) Filamentous actin in association with phagosomes was quantified by measuring pixel intensities on images of beads collected in the green channel. Error bars, SD (n = 10). (F) Phagosome-associated lysosomes were quantified by measuring pixel intensities on images of beads collected in the red channel. Error bars, SD (n = 20).

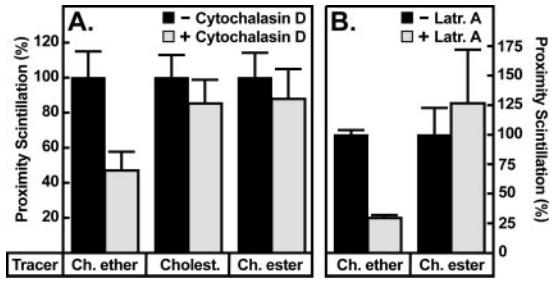

Figure 7. Actin polymerization is required for phagosome maturation in vivo. (A and B) Live-cell scintillation proximity assays. On day 0, J774 macrophages cells were set up in a white opaque 24-well plate at 10^5 cells/well in 1 ml of medium A. On day 1, each well received 50 μg of scintillant YSi beads in 0.5 ml of medium B. After 45 min of phagocytosis at 37°C, the medium was changed to 0.5 ml medium B in the absence or presence of 10 μM cytochalasin D or 1 μM latrunculin A (Latr. A) as indicated. Cells were incubated on ice for 15 min and then received liposomes containing [^{3}H]cholesteryl oleoyl ether (Ch. ether), [^{3}H]cholesteryl oleoyl ester (Ch. ester) or [^{3}H]cholesterol (Cholest.; 1 nCi/0.5 ml/well). After 4 h at 37°C, cells were washed three times with PBS and proximity scintillation was measured in a Packard model Topcount microplate scintillation reader. Subsequently, cells were harvested into 100 μl PBS containing 0.1% Triton X-100 and total radioactivity was determined by liquid scintillation counting. Proximity scintillation was divided by total radioactivity and data are plotted as percentage with respect to controls. Error bars, SD (n = 3).

The results in Figure 5, A and B, support a scheme in which the initial attachment process under Ca^{2+}-free conditions can be further divided into two stages. Stage one, operationally referred to as tethering, involves actin polymerization. During stage two, here referred to as docking, ongoing actin polymerization is no longer required but the complex remains sensitive to alkaline carbonate. Apparently, during the subsequent Ca^{2+}-induced consolidation phase, actin polymerization is also not required.

To further explore the role of actin polymerization during lysosome/phagosome attachment we tested the effect of phalloidin, a drug that prevents the de-polymerization of filamentous actin (Cooper, 1987). Under Ca^{2+}-free reaction conditions phalloidin led to a threefold increase of the scintillation signal with respect to controls (Figure 5C).

As a validation for the cell-free scintillation proximity assay, in vitro reaction products were analyzed by fluorescence microscopy. The experimental setup was identical to that used above, except that lysosomes were labeled with a fluorescent fluid-phase marker, Alexa 594 hydrazide (Panchuk-Voloshina *et al.*, 1999; Yates *et al.*, 2005), and reactions were supplemented with FITC-labeled actin. As shown in Figure 6, A–D, tufts of actin on the surface of phagosomes and lysosomes were formed in an ATP-dependent manner. In the presence of ATP, phagosomes were often seen in association with lysosomes (panels B–D). Lysosomes were seen either tethered via actin (panel B) or in close contact with phagosomes (panels C and D).

Results similar to those obtained with FITC-actin were obtained when filamentous actin was labeled with FITC-phalloidin (unpublished data). After phalloidin staining, quantification of pixel intensity indicated that ATP led to a 2.5-fold increase of phagosome-associated filamentous actin (Figure 6E; $p < 0.0003$) and to an 8200-fold increase of phagosome-associated Alexa 594 fluorescence (Figure 6F; $p < 0.042$).

The results in Figures 5 and 6 support the conclusion that the role of actin polymerization during lysosome/phagosome interactions is to facilitate the formation of a prefusion complex. To verify this conclusion under more physiological conditions, scintillation proximity assays were performed in vivo. We have previously shown that incubation of living macrophages with scintillant yttrium silicate beads and tritiated lipids leads to light emission in a phagocytosis-dependent manner (Stockinger *et al.*, 2004). In Figure 7 we used this assay to study the effects of actin inhibitors on the interaction of phagosomes with endosomes and lysosomes. J774 macrophages were first incubated with yttrium silicate for 45 min, which is enough to saturate the cells with beads. The cells then received [^{3}H]cholesteryl ether–fortified liposomes for an additional 4 h before being analyzed for proximity scintillation. To eliminate variations in the uptake of liposomes, proximity scintillation was corrected for total cellular radioactivity. When cytochalasin D was added together with [^{3}H]cholesteryl ether, specific proximity scintillation was reduced by 53% (Figure 7A). Similar results were seen with latrunculin A (Figure 7B).

Although the drugs were added 45 min after the start of phagocytosis, the specific proximity scintillation could have been reduced because of inhibition of continuing particle

uptake (de Oliveira and Mantovani, 1988). To rule out this possibility, some cells were also labeled with [^{3}H]cholesterol. Whereas cholesteryl ether remains membrane-bound, cholesterol readily exchanges by diffusion (Frolov *et al.*, 1996; Wang *et al.*, 2005), and the movement of cholesterol to phagosomes should be independent of membrane fusion (Liscum, 1990). In fact, after labeling cells with [^{3}H]cholesterol, cytochalasin D had no effect (Figure 7A). Both drugs were also innocuous in cells labeled with [^{3}H]cholesteryl ester, which is hydrolyzed to [^{3}H]cholesterol in endosomes and lysosomes (Figure 7, A and B). Collectively, the results in Figures 5–7 support the conclusion that lysosome/phagosome attachment requires actin polymerization.

Lysosome/Phagosome Attachment Requires Calmodulin

The sensitivity of lysosome/phagosome interactions to Ca^{2+} suggests that the cytosolic docking and fusion machinery contains one or more Ca^{2+}-sensing proteins. One candidate is calmodulin, inhibitors of which have previously been shown to interfere with phagosome maturation in vivo (Brewton and MacCabe, 1988; Sionov and Gallily, 1990; Malik *et al.*, 2001; Vergne *et al.*, 2003; Yates *et al.*, 2005). Analysis of in vitro reaction products shows calmodulin staining in association with both lysosomes and phagosomes (Figure 8A) that was dependent on ATP (unpublished data). In Figure 8, B–F, we studied the effects of different calmodulin inhibitors in the cell-free scintillation proximity assay. Under low Ca^{2+} reaction conditions, W7, trifluoperazine, and calmidazolium inhibited docking in a concentration-dependent manner (Figure 8, B–D). W5, a de-chlorinated and less potent analog of W7 (Hidaka *et al.*, 1981), was without effect (Figure 8B).

We then asked at what stage of the docking and fusion process calmodulin is required. To address this question, W7 was added at the beginning or only during the second half of a two-phase scintillation proximity assay. When W7 was added from the start of the reaction, scintillation was blocked (Figure 8E, reaction b, black bar). When W7 was added only during phase 2, the scintillation signal remained high (reaction c, black bar). Moreover, addition of W7 together with Ca^{2+}during phase 2, failed to prevent the formation of a carbonate-resistant complex (reaction f). Similar results were obtained with trifluoperazine (Figure 8F). The results in Figure 8 thus suggest that tethering of lysosomes to phagosomes in vitro requires calmodulin. During docking and consolidation, calmodulin appears to be dispensable.

To study the role of calmodulin in living cells, RAW macrophages were exposed to latex beads after labeling lysosomes with fluorescent dextran. After 1 h of phagocytosis cells were fixed and stained with filipin. Under control conditions, filipin-marked phagosomes displayed rings of continuous dextran fluorescence, indicating that lysosomes and phagosomes had fused (Figure 9A, rows 1 and 2). By contrast, in the presence of W7 or trifluoperazine, phagosome-associated dextran fluorescence was significantly reduced (Figure 9A, rows 3 and 4).

As a more quantitative approach to studying the effects of W7 and trifluoperazine in vivo, we performed a live-cell scintillation proximity assay. J774 macrophages were exposed to scintillant yttrium silicate beads for 45 min and subsequently received [^{3}H]cholesteryl ether plus or minus drugs for an additional 4 h. We then determined proximity scintillation corrected for total cellular radioactivity. In response to W7 and trifluoperazine, specific proximity scintillation was reduced by 55 and 69%, respectively (Figure 9, B and C, black bars). W5 had little effect. No reduction of the specific proximity scintillation was observed in cells labeled with [^{3}H]cholesteryl ester (gray bars). Taken together, the results in Figures 8 and 9 are consistent with the conclusion that calmodulin is required for lysosome/phagosome attachment.

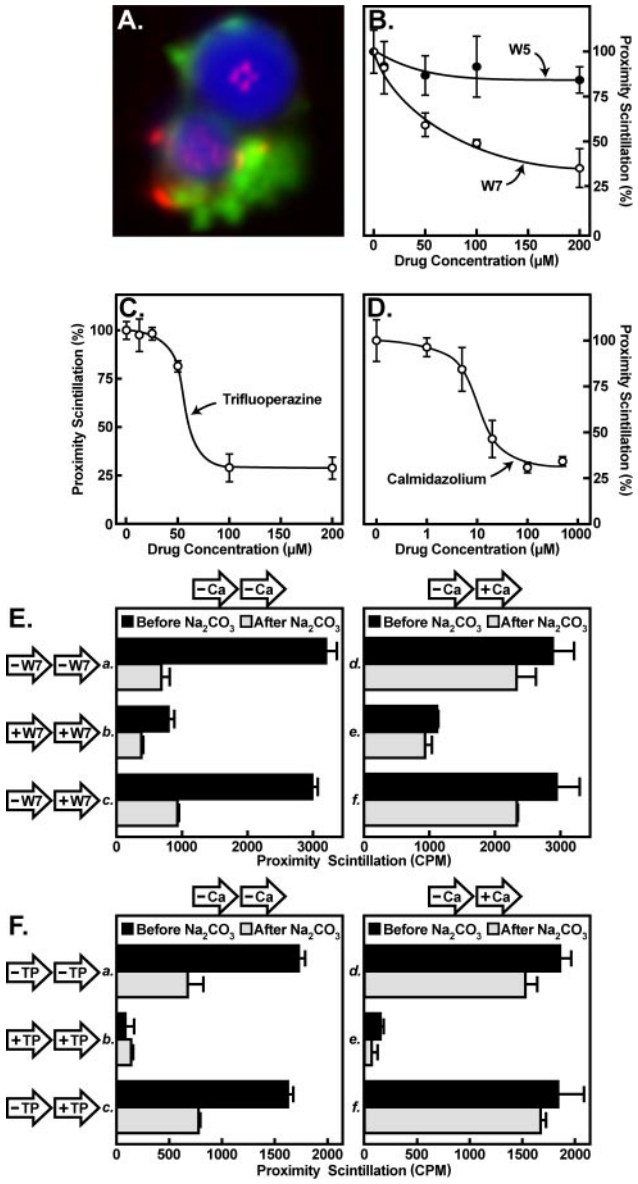

Figure 8. Lysosome/phagosome docking is sensitive to calmodulin inhibitors. (A) In vitro docking reactions were performed as in Figure 6, A–D, and lysosomes were labeled with Alexa Fluor 594 hydrazide. Reaction products were then fixed, and calmodulin was detected with a polyclonal antibody plus an Alexa Fluor 488 tyramide detection system. Samples were analyzed by confocal fluorescence microscopy. Blue, PVT beads; green calmodulin; red, lysosomes. (B–D) In vitro reactions were set up as in Figure 1A plus the indicated concentrations of W5, W7, trifluoperazine, and calmidazolium, incubated for 1 h at 37°C, and analyzed for proximity scintillation. Data represent scintillation counts with respect to samples incubated without inhibitor. (E) Two-step in vitro reactions were performed as in Figure 3B. Left, all reactions were performed in the absence of Ca^{2+}; right, 2 mM Ca^{2+} was added during phase 2. W7 (150 μM) was present during phase 1 and phase 2 or only during phase 2 where indicated. Proximity scintillation was determined before (black bars) and after (gray bars) sodium carbonate treatment as in Figure 2. (E) Two-step reactions were performed as in F, except that 100 μM trifluoperazine (TP) was used instead of W7. Error bars, SD (n = 2).

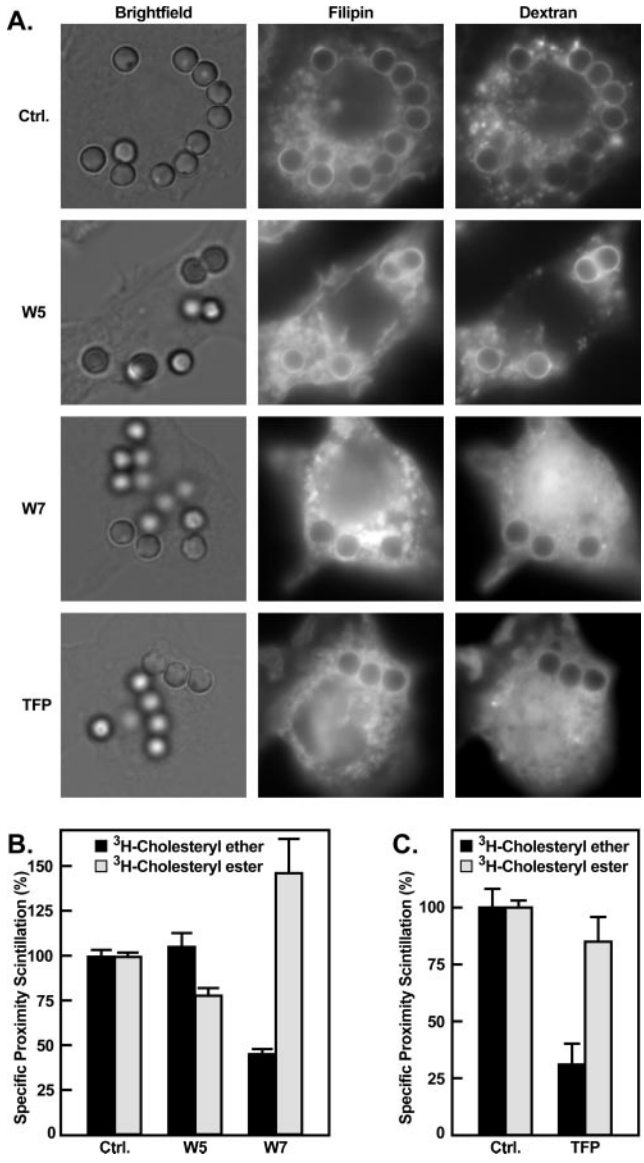

Figure 9. Calmodulin inhibitors interfere with phagosome maturation in vivo. (A) RAW cells were set up as in Figure 4. On day 1, the medium was changed to medium A containing 0.1 mg/ml fixable tetramethyl rhodamine-dextran (10 kDa, Invitrogen). On day 2, cells were washed and incubated for 30 min with fresh medium A. Each well then received 25 μg of 3-μm IgG-conjugated latex beads and plates were centrifuged for 2 min at 1000 $\times$ *g*. Subsequently, cells were incubated at 37°C for 3 min to allow for phagocytosis, washed, and switched to fresh medium. Media were supplemented with solvent (Ctrl.), 50 μM W5, W7, or trifluoperazine (TFP), and placed on ice for 15 min. The temperature was raised again to 37°C for 60 min. Subsequently, the cells were washed with PBS, fixed with 4% paraformaldehyde, stained with 50 μg/ml filipin, mounted on glass slides, and analyzed with an inverted microscope as in Figure 4. (B and C) Live-cell scintillation proximity assays. J774 cells were set up as in Figure 7. On day 1 each well received 50 μg scintillant YSi beads in 0.5 ml of medium B. After 45 min of phagocytosis at 37°C, the medium was changed to 0.5 ml medium B plus 50 μM W5, W7 or trifluoperazine (TFP) where indicated. Cells were incubated on ice for 15 min and then received liposomes containing [^{3}H]cholesteryl oleoyl ether (black bars) or [^{3}H]cholesteryl oleoyl ester (gray bars; 1 nCi/0.5 ml/well). After 4 h at 37°C proximity scintillation was determined as in Figure 7. Error bars, SD (n = 3).

Cytosol Fractionation Studies

Next, the cytosolic activity required for lysosome/phagosome docking was followed through several purification steps. Rat liver cytosol was sequentially subjected to ammonium sulfate precipitation, hydrophobic interaction chromatography and a DEAE anion exchange column. Elution fractions were analyzed in the cell-free docking assay. After ammonium sulfate precipitation and hydrophobic interaction chromatography the activity peaked several-fold above background (unpublished data). By contrast, only a low peak in fractions 13–15 was observed after elution from the DEAE column, indicating that the protein(s) had been denatured or that a protein complex had separated during chromatography (Figure 10A). In the latter case, the fractions with low activity might represent a region of partial overlap between two neighboring factors, both of which would be required for maximal attachment. Indeed, when all eluates were retested in the presence of fraction 15, a clear peak was seen in fraction 11 (Figure 10B). Conversely, when the eluates were assayed in the presence of fraction 11, a well-defined peak was observed in fraction 15 (Figure 10C). The activities in fractions 11 and 15 were designated as factor A and factor B, respectively.

Following up on our inhibitor studies, the DEAE fractions were then analyzed by immunoblotting with antibodies directed against actin and calmodulin. Factor A copurified with actin (Figure 10D) and factor B copurified with calmodulin (Figure 10E).

To test whether purified actin and calmodulin are sufficient to replace rat liver cytosol, docking reactions were supplemented with purified proteins from commercial sources. Even in combination, actin and calmodulin had no effect (Figure 10F, reaction 5). However, when added to rat liver cytosol, there was about a twofold increase of the proximity scintillation signal (Figure 10F, compare reactions 2 and 6). These results indicate that one or more additional proteins must be required for lysosome/phagosome attachment.

To continue purification, factor A was subjected to hydroxyapatite chromatography, and elution fractions were assayed in combination with factor B (Figure 10G). SDS-PAGE followed by Coomassie staining identified two major bands of ~40 and 120 kDa whose intensity patterns matched the activity profile (Figure 10H). Based on Western blotting and comigration with an authentic standard, the 40-kDa band was identified as actin (Figure 10H, closed arrows). Using microcapillary HPLC tandem mass spectrometry the 120-kDa band was identified as ubiquitin-activating enzyme (E1) (Figure 10H, open arrow).

Factor B, following DEAE chromatography, was subjected to gel filtration and eluates were assayed for docking activity in combination with factor A (Figure 10I). The peak of activity eluted at a molecular weight of ~550 kDa. Fractions were also analyzed by SDS-PAGE and silver staining, identifying two major bands of 17 and 180 kDa that peaked in the same fraction as the docking activity (Figure 10J). Both bands were sequenced by mass spectrometry and identified as calmodulin and IQGAP2, respectively.

IQGAP2 belongs to a family of actin cross-linking proteins that form a core complex with calmodulin and the small G proteins Cdc42 or Rac1 (Briggs and Sacks, 2003). Similar to the current gel filtration profile, human IQGAP1 was found to elute from gel filtration columns at ~600 kDa, suggesting the presence of 2 or 3 IQGAP molecules in the complex (Fukata *et al.*, 1997). The molecular weight of Cdc42 and Rac1 is ~21 kDa, but a band of that size did not stand out after silver staining (Figure 10J). However, our mass spectrometry data obtained

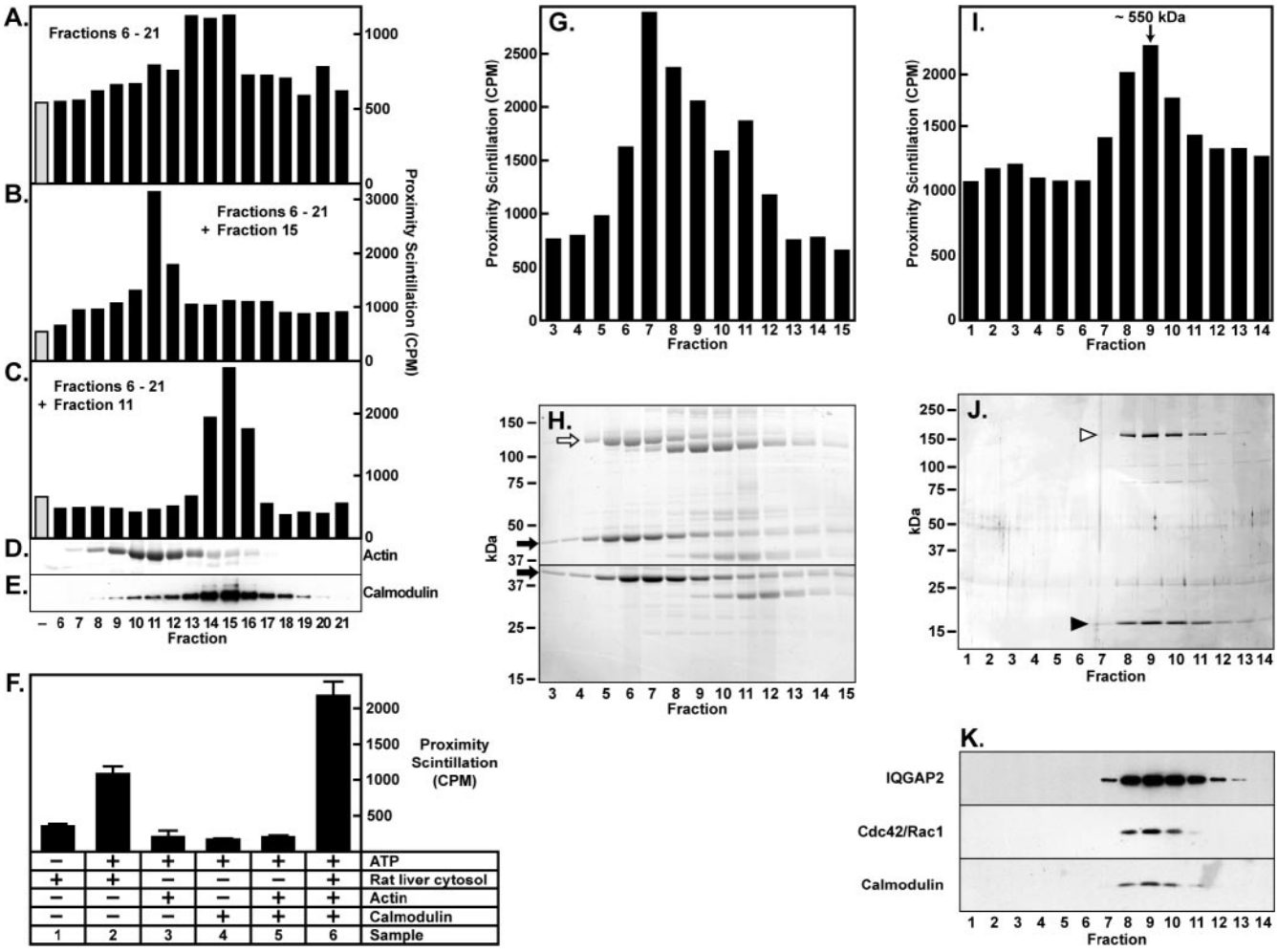

Figure 10. Purification of cytosolic docking activity. Cytosol from the livers of four rats was pooled and subjected to an ammonium sulfate cut between 1.2 M and 1.8 M, and the resulting pellet dissolved in 20 ml of buffer C. This solution was loaded on a 20-ml phenyl sepharose HP column (GE Healthcare) and eluted at a flow rate of 1 ml/min with a linear gradient of ammonium sulfate (0.7 M to 0 M) and polyethyleneglycol (0–50%) in buffer C. Thirty 10-ml fractions were collected and dialyzed twice against 1 l of buffer D overnight at 4°C. The fractions were then analyzed in the cell-free scintillation proximity assay. The highest activity was found in fractions 15–19, which were pooled, loaded on a 5-ml DEAE Sepharose FF column (GE Healthcare) and eluted at a flow rate of 0.5 ml/min in buffer E by gradually increasing the concentration of KCl from 50 to 250 mM. Fractions of 2.5-ml were collected and each was dialyzed three times against buffer B containing 250 mM sucrose. (A) Fractions 6–21 of the DEAE eluate were analyzed in the cell-free scintillation proximity assay. (B) Fractions 6–21 of the DEAE eluate were individually combined with fraction 15 and analyzed in the cell-free scintillation proximity assay. (C) Fractions 6–21 of the DEAE eluate were individually combined with fraction 11 and analyzed in a cell-free scintillation proximity assay. (D and E) Fractions 6–21 of the DEAE eluate were subjected to SDS-PAGE, transferred to nitrocellulose, and blotted with antibodies (D) against actin and (E) against calmodulin. (F) Cell-free docking assays were performed for 1 h as in Figure 1A, except that some reactions received 50 μg/ml purified nonmuscle actin and/or 500 μg/ml purified calmodulin. (G) DEAE fractions positive for factor A activity were pooled and dialyzed against buffer G, and 5 ml were loaded on a 1-ml hydroxyapatite column (Sigma H0252). Proteins were eluted at a flow rate of 0.3 ml/min with a linear gradient of buffer B (0–100%), and 0.3-ml fractions were collected. Fractions of 50 μl were combined with 100 μl of factor B from a DEAE column and analyzed for docking activity as above. (H) The same hydroxyapatite eluates analyzed in G were applied to 10% SDS-PAGE and stained with Coomassie Blue. Because of warping, the upper and lower parts of the gel were scanned separately. The open arrow denotes E1; the closed arrows denote actin. (I) DEAE fractions positive for factor B were pooled, 3 ml was concentrated three times with a 30-kDa cutoff centrifugation filter (Amicon, Beverly, MA) and then separated in buffer G on a HiPrep 16/60 Sephacryl S-300 gel filtration column (GE Healthcare) at a flow rate of 0.5 ml/min, and 1-ml fractions were collected. Then 190 μl of each fraction was combined with 65 μl of factor A from a DEAE column and analyzed for docking activity as above. (J) The same gel filtration eluates analyzed in I were applied to 7–17% SDS-PAGE and silver-stained. The open arrowhead denotes IQGAP2, and the closed arrowhead denotes calmodulin. (K) The same fractions analyzed in I and J were separated by SDS-PAGE, transferred to nitrocellulose, and blotted with antibodies against IQGAP2, Cdc42/Rac1, and calmodulin as indicated. Purification data are summarized in Table 1.

from the calmodulin band included five peptide ions derived from Cdc42 (unpublished data). In fact, when the gel filtration fractions were analyzed by Western blotting with a dual-specificity antibody against Cdc42 and Rac1, a band of the appropriate size was found to coelute with calmodulin and IQGAP2 (Figure 10K). Possibly, a fraction of IQGAP2-bound Cdc42/Rac1 was lost during gel filtration, which might in part explain the relatively low activity of the eluate (Figure 10I).

Taken together, the results in Figure 10 further support the conclusion that lysosome/phagosome attachment re-

Table 1. Purification of proximity scintillation activity from rat liver cytosol

Purification step	Volume (ml)	Protein (mg)	Total activity (CPM)	Specific activity (CPM/mg protein)	Purification (-fold)	Recovery (%)
Cytosol	40	1,840	514,286	280	1	100
Ammonium sulfate precipitation	40	340	ND	ND	ND	ND
Hydrophobic interaction chromatography	47	23.5	397,692	16,923	60	77
Factor A						
DEAE column	7.5	0.75	67,667	90,222	322	13
Hydroxyapatite column[a]	0.6	0.018	18,075	1004,167	3,586	4
Factor B						
DEAE column	7.5	0.75	96,218	128,291	458	19
Gel filtration[b]	2	0.06	47,529	792,150	2,829	9

Activity refers to summative proximity scintillation (in CPM) in active fractions after correction for the background signal. Factor A activities were assayed in combination with aliquots of DEAE eluates containing factor B and the activity after hydroxyapatite chromatography refers to fractions 6 and 7 in Figure 10G. Factor B activities were assayed in combination with aliquots of DEAE eluates containing factor A and the activity after gel filtration refers to fractions 8 and 9 in Figure 10I. ND, not determined.

quires actin and calmodulin and they suggest that calmodulin can act in a complex with IQGAP and Cdc42/Rac1 to mediate the cross-linking of actin filaments.

DISCUSSION

It is now well established that the fusion of vesicles with target membranes proceeds in three broadly defined phases (Pfeffer, 1999; Mellman and Warren, 2000). During phase 1, often referred to as "tethering," membranes become attached via cytosolic proteins that leave the membranes at a distance of 25 nm or greater. In phase 2, sometimes called "docking," bilayers are brought into almost direct contact. At the end of phase 3 the bilayers fuse.

In the current article, evidence is presented that similar to other cellular targeting events, lysosomes/phagosome interactions proceed through tethering and docking steps. In addition, we show that actin polymerization and calmodulin are required for the early tethering process, but not at later stages of the targeting pathway; conversely, postdocking events appear to require Ca^{2+}, whereas tethering and docking occur in the absence of Ca^{2+} (summarized in Figure 11).

In support of the concept that tethering and docking precede fusion we found that isolated lysosomes and phagosomes attach to each other in a reaction dependent on physiological temperature, ATP and proteins from rat liver cytosol (Figures 1 and 10). In most experiments lysosomes were added in postnuclear supernatant fractions, of which both the membrane and cytosol components are required to produce a scintillation signal (Trivedi, V., Zhang, S. C., Stockinger, W., Shieh, E. and Nohturfft, A., unpublished data). The nascent complex is characterized by being resistant to high salt but sensitive to alkaline carbonate (Figure 2). Because carbonate disrupts protein interactions while leaving bilayers and cholesteryl ether localization intact (Fujiki *et al.*, 1982 and Figure 2), we conclude that the early phase of the targeting process arrests at a stage, here referred to as "docked," where lysosomes and phagosomes have not yet fused.

In vivo evidence for docked intermediates comes from microscopy data showing phagosomes studded with vesicles containing the late endosomal/lysosomal marker Lamp2 (Figure 4). The alternative interpretation that the uneven fluorescence might be an artifact of antibody staining is ruled out by two additional observations: 1) after 4 h of phagocytosis or later, Lamp2 staining around phagosomes was uniformly smooth and ring-shaped, indicating that the docked vesicles represent an intermediate in the maturation process; 2) results similar to those obtained with a Lamp2 antibody were obtained when lysosomes were marked by fluorescent dextran or by transfection of cells with a Lamp1-RFP fusion construct (unpublished data).

The concept that docking is attained via a tethered intermediate is based on series of 2-h in vitro experiments where the reaction conditions were varied between the first and second half of the incubation period. Three reagents were found to block the reaction when added from the start: 1) inhibitors of actin polymerization (Figure 5), 2) calmodulin inhibitors (Figure 8), and 3) micro to millimolar concentrations of Ca^{2+} (Figure 3 and unpublished data). In contrast, when reactions were allowed to proceed under control con-

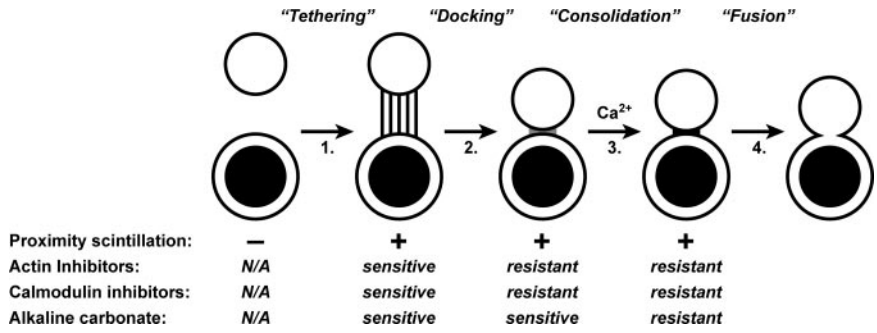

Figure 11. Model for lysosome/phagosome targeting. In step 1, lysosomes and phagosomes are tethered in a process requiring actin polymerization and calmodulin. Step 2 results in formation of a complex that is resistant to inhibitors of calmodulin and actin polymerization but sensitive to alkaline carbonate. Step 3 is triggered by an increase in the Ca^{2+} concentration and leads to formation of an alkali-resistant complex. In step 4 bilayers fuse. Note that content mixing between lysosomes and phagosomes was not assayed in this article.

ditions for 1 h and drugs or Ca^{2+} were added only during the second incubation step, the scintillation signal remained unchanged. We interpret these results to indicate that calmodulin and F-actin mediate tethering of lysosomes to phagosomes where tethering is a transient process that precedes formation of the docked configuration. For the stability of docked complexes calmodulin and ongoing actin polymerization are no longer required. These results are broadly reminiscent of studies on chromaffin cells where filamentous actin helps in tethering secretory vesicles to the cell cortex but disassembles before fusion (Trifaro and Vitale, 1993).

Our results that actin inhibitors block tethering are in accordance with earlier studies showing that endosomes, lysosomes, and phagosomes can aggregate via actin bundles and that actin polymerization facilitates their fusion (van Deurs *et al.*, 1995; Jahraus *et al.*, 2001; Kjeken *et al.*, 2004). Actin filament formation can initiate on the surface of endosomes, lysosomes, and phagosomes (Taunton *et al.*, 2000; Jahraus *et al.*, 2001; Kjeken *et al.*, 2004) and during yeast vacuole fusion F-actin localizes to the vertex ring at the docking stage (Eitzen *et al.*, 2002). In contrast to lysosome/phagosome targeting, inhibition of actin polymerization in yeast blocks the fusion of vacuoles but does not affect docking (Eitzen *et al.*, 2002).

Kjeken *et al.* (2004) have shown and our microscopy data in Figure 6 confirm that actin filaments remain associated with phagosomes beyond the time required for docking. However, the fact that the docking complex, once formed, remains stable during 1-h incubations with inhibitors of actin polymerization opens the possibility that F-actin is no longer required. On the other hand, depolymerization by latrunculin A and cytochalasin D requires treadmilling, and it is conceivable that docking coincides with filament stabilization through association with capping proteins.

In the simplest model for actin-mediated tethering, interacting vesicles zipper up via actin cross-linking proteins and our demonstration that IQGAP2 can mediate lysosome/phagosome attachment in vitro supports such a model. IQGAP2 is a member of a family of actin cross-linking proteins that are conserved from yeast to humans (Briggs and Sacks, 2003). The principal features of IQGAP2 and its closest homolog, IQGAP1 (62% identical), include an N-terminal calponin homology domain (CHD) that can bind F-actin, four calmodulin-binding IQ motifs, and a GTPase-activating protein (GAP)-related domain (GRD) that can bind Cdc42 or Rac1. The C-terminus can mediate binding to E-cadherin and β-catenin and to microtubules via CLIP-170. Similar to other IQ motif proteins (Jurado *et al.*, 1999), IQGAPs bind calmodulin in the absence of Ca^{2+}, but interactions are enhanced in the presence of Ca^{2+} (Li and Sacks, 2003). Despite their GRD domains IQGAP1 and IQGAP2 have no GAP activity but stabilize the GTP-bound form of Cdc42 and Rac1 (Briggs and Sacks, 2003). Binding of GTP-Cdc42/Rac1 in turn is required for the ability of IQGAP1 to cross-link F-actin into bundles and gels (Bashour *et al.*, 1997; Fukata *et al.*, *1997).*

During our cytosol fractionation studies we found that the IQGAP2 complex had to be combined with fractions containing both actin and E1 (Figure 10). Although a requirement for actin is in agreement with our inhibitor studies, an involvement of E1 is not yet supported by other data. E1 catalyzes the first step in the ubiquitylation cascade (Hershko and Ciechanover, 1998) and a large number of phagosomal proteins are ubiquitylated (Lee *et al.*, 2005). However, in CHO cells with a temperature-sensitive E1 mutation lysosome/phagosome fusion is unaffected (Booth *et al.*, 2002).

In our cell-free assay docked complexes of lysosomes and phagosomes are stable but remain sensitive to disruption even after several hours of incubation. However, when reactions were allowed to dock first and then exposed to Ca^{2+}, the interactions then became resistant to alkaline carbonate (Figures 3, 5, and 8). The high extent of carbonate resistance suggests that Ca^{2+}-induced consolidation is initiated at a step upstream of fusion. Analogously, in an assay measuring content mixing between late endosomes and lysosomes, the first Ca^{2+} requiring step was found to precede fusion by at ~5 min (Pryor *et al.*, 2000).

Generation of carbonate-resistant lysosome/phagosome complexes must be performed in two steps because when Ca^{2+} is present from the beginning of the reaction even docking is blocked (Figure 3). In this context it is interesting to note that Ca^{2+} has been shown to disrupt the ability of IQGAP1 to cross-link F-actin (Ho *et al.*, 1999; Mateer *et al.*, 2002), suggesting that IQGAP2 might have been responsible for mediating the differential Ca^{2+} effects during our in vitro reactions.

In vitro, the half-maximal Ca^{2+} concentration required for acquisition of carbonate resistance lies between 1 and 10 μM (Figure 3), which is similar to results obtained for Ca^{2+}-mediated fusion events in vivo (Jaconi *et al.*, 1990; Burgoyne and Clague, 2003) and during late endosome/lysosome fusion and yeast vacuole fusion in vitro (Peters and Mayer, 1998; Pryor *et al.*, 2000). In previous studies the Ca^{2+} dependence during endosome fusion assays was found to be bell-shaped (Peters and Mayer, 1998; Holroyd *et al.*, 1999; Pryor *et al.*, 2000), whereas Ca^{2+}-induced consolidation in our scintillation proximity assay is sigmoidal (Figure 3). If our current results extend to other systems and Ca^{2+} blocks tethering while promoting the fusion of vesicles that have already docked, optimal Ca^{2+} concentrations in single-step fusion reactions might potentially reflect a synthesis between least inhibition and maximal consolidation.

The concept that the early and late steps of lysosome/phagosome targeting are regulated differently by Ca^{2+} makes physiological sense because the cytosolic Ca^{2+} concentration is usually very low. That way, lysosomes and phagosomes can attach under resting conditions and remain docked until Ca^{2+} spikes trigger subsequent targeting steps.

ACKNOWLEDGMENTS

We are grateful to Johann Bollmann, Tim Mitchison, Andrew Murray, Venkatesh Murthy, and David Sacks for helpful discussions. This work was supported by National Institutes of Health Grant R01 DK59934 (A.N.). W.S. was supported through fellowships from the Max Kade Foundation and the Austrian Academy of Sciences.

REFERENCES

Aikawa, K., Furuchi, T., Fujimoto, Y., Arai, H., and Inoue, K. (1994). Structure-specific inhibition of lysosomal cholesterol transport in macrophages by various steroids. Biochim. Biophys. Acta *1213*, 127–134.

Bajno, L., Peng, X. R., Schreiber, A. D., Moore, H. P., Trimble, W. S., and Grinstein, S. (2000). Focal exocytosis of VAMP3-containing vesicles at sites of phagosome formation. J. Cell Biol. *149*, 697–706.

Bashour, A. M., Fullerton, A. T., Hart, M. J., and Bloom, G. S. (1997). IQGAP1, a Rac- and Cdc42-binding protein, directly binds and cross-links microfilaments. J. Cell Biol. *137*, 1555–1566.

Blocker, A., Griffiths, G., Olivo, J. C., Hyman, A. A., and Severin, F. F. (1998). A role for microtubule dynamics in phagosome movement. J. Cell Sci. *111 (Pt* 3), 303–312.

Booth, J. W., Kim, M. K., Jankowski, A., Schreiber, A. D., and Grinstein, S. (2002). Contrasting requirements for ubiquitylation during Fc receptor-mediated endocytosis and phagocytosis. EMBO J. *21*, 251–258.

Bornig, H., and Geyer, G. (1974). Staining of cholesterol with the fluorescent antibiotic "filipin." Acta Histochem. *50*, 110–115.

Braun, V., Fraisier, V., Raposo, G., Hurbain, I., Sibarita, J. B., Chavrier, P., Galli, T., and Niedergang, F. (2004). TI-VAMP/VAMP7 is required for optimal phagocytosis of opsonised particles in macrophages. EMBO J. *23*, 4166–4176.

Brewton, R. G., and MacCabe, J. A. (1988). In vitro effects of calmodulin antagonists on macrophage function in the posterior necrotic zone of the chick wing. J. Exp. Zool. *246*, 103–107.

Briggs, M. W., and Sacks, D. B. (2003). IQGAP1 as signal integrator: Ca2+, calmodulin, Cdc42 and the cytoskeleton. FEBS Lett. *542*, 7–11.

Brown, M. S., and Goldstein, J. L. (1976). Analysis of a mutant strain of human fibroblasts with a defect in the internalization of receptor-bound low density lipoprotein. Cell *9*, 663–674.

Burgoyne, R. D., and Clague, M. J. (2003). Calcium and calmodulin in membrane fusion. Biochim. Biophys. Acta *1641*, 137–143.

Castellano, F., Chavrier, P., and Caron, E. (2001). Actin dynamics during phagocytosis. Semin. Immunol. *13*, 347–355.

Chen, J. W., Murphy, T. L., Willingham, M. C., Pastan, I., and August, J. T. (1985). Identification of two lysosomal membrane glycoproteins. J. Cell Biol. *101*, 85–95.

Cooper, J. A. (1987). Effects of cytochalasin and phalloidin on actin. J. Cell Biol. *105*, 1473–1478.

Daleke, D. L., Hong, K., and Papahadjopoulos, D. (1990). Endocytosis of liposomes by macrophages: binding, acidification and leakage of liposomes monitored by a new fluorescence assay. Biochim. Biophys. Acta *1024*, 352–366.

de Duve, C. (1963). The lysosome concept. In: Lysosomes, ed. A.V.S. de Reuck and M. P. Cameron, London: Churchill, 1–35.

de Oliveira, C. A., and Mantovani, B. (1988). Latrunculin A is a potent inhibitor of phagocytosis by macrophages. Life Sci. *43*, 1825–1830.

Defacque, H., Bos, E., Garvalov, B., Barret, C., Roy, C., Mangeat, P., Shin, H. W., Rybin, V., and Griffiths, G. (2002). Phosphoinositides regulate membrane-dependent actin assembly by latex bead phagosomes. Mol. Biol. Cell *13*, 1190–1202.

Defacque, H., Egeberg, M., Habermann, A., Diakonova, M., Roy, C., Mangeat, P., Voelter, W., Marriott, G., Pfannstiel, J., Faulstich, H., and Griffiths, G. (2000). Involvement of ezrin/moesin in de novo actin assembly on phagosomal membranes. EMBO J. *19*, 199–212.

Desjardins, M., Huber, L. A., Parton, R. G., and Griffiths, G. (1994). Biogenesis of phagolysosomes proceeds through a sequential series of interactions with the endocytic apparatus. J. Cell Biol. *124*, 677–688.

Dunn, W. A., Connolly, T. P., and Hubbard, A. L. (1986). Receptor-mediated endocytosis of epidermal growth factor by rat hepatocytes: receptor pathway. J. Cell Biol. *102*, 24–36.

Dunn, W. A., Hubbard, A. L., and Aronson, N. N., Jr. (1980). Low temperature selectively inhibits fusion between pinocytic vesicles and lysosomes during heterophagy of 125I-asialofetuin by the perfused rat liver. J. Biol. Chem. *255*, 5971–5978.

Eitzen, G., Wang, L., Thorngren, N., and Wickner, W. (2002). Remodeling of organelle-bound actin is required for yeast vacuole fusion. J. Cell Biol. *158*, 669–679.

Frolov, A., Woodford, J. K., Murphy, E. J., Billheimer, J. T., and Schroeder, F. (1996). Spontaneous and protein-mediated sterol transfer between intracellular membranes. J. Biol. Chem. *271*, 16075–16083.

Fujiki, Y., Hubbard, A. L., Fowler, S., and Lazarow, P. B. (1982). Isolation of intracellular membranes by means of sodium carbonate treatment: application to endoplasmic reticulum. J. Cell Biol. *93*, 97–102.

Fukata, M., Kuroda, S., Fujii, K., Nakamura, T., Shoji, I., Matsuura, Y., Okawa, K., Iwamatsu, A., Kikuchi, A., and Kaibuchi, K. (1997). Regulation of cross-linking of actin filament by IQGAP1, a target for Cdc42. J. Biol. Chem. *272*, 29579–29583.

Gilmore, R., and Blobel, G. (1985). Translocation of secretory proteins across the microsomal membrane occurs through an environment accessible to aqueous perturbants. Cell *42*, 497–505.

Hart, H. E., and Greenwald, E. B. (1979). Scintillation proximity assay (SPA)—a new method of immunoassay. Direct and inhibition mode detection with human albumin and rabbit antihuman albumin. Mol. Immunol. *16*, 265–267.

Hershko, A., and Ciechanover, A. (1998). The ubiquitin system. Annu. Rev. Biochem. *67*, 425–479.

Hidaka, H., Sasaki, Y., Tanaka, T., Endo, T., Ohno, S., Fujii, Y., and Nagata, T. (1981). N-(6-aminohexyl)-5-chloro-1-naphthalenesulfonamide, a calmodulin antagonist, inhibits cell proliferation. Proc. Natl. Acad. Sci. USA *78*, 4354–4357.

Ho, Y. D., Joyal, J. L., Li, Z., and Sacks, D. B. (1999). IQGAP1 integrates Ca2+/calmodulin and Cdc42 signaling. J. Biol. Chem. *274*, 464–470.

Holroyd, C., Kistner, U., Annaert, W., and Jahn, R. (1999). Fusion of endosomes involved in synaptic vesicle recycling. Mol. Biol. Cell *10*, 3035–3044.

Jaconi, M. E., Lew, D. P., Carpentier, J. L., Magnusson, K. E., Sjogren, M., and Stendahl, O. (1990). Cytosolic free calcium elevation mediates the phagosome-lysosome fusion during phagocytosis in human neutrophils. J. Cell Biol. *110*, 1555–1564.

Jahraus, A., Egeberg, M., Hinner, B., Habermann, A., Sackman, E., Pralle, A., Faulstich, H., Rybin, V., Defacque, H., and Griffiths, G. (2001). ATP-dependent membrane assembly of F-actin facilitates membrane fusion. Mol. Biol. Cell *12*, 155–170.

Jurado, L. A., Chockalingam, P. S., and Jarrett, H. W. (1999). Apocalmodulin. Physiol. Rev. *79*, 661–682.

Kjeken, R. *et al.* (2004). Fusion between phagosomes, early and late endosomes: a role for actin in fusion between late, but not early endocytic organelles. Mol. Biol. Cell *15*, 345–358.

Lange, Y., Ye, J., and Steck, T. L. (1998). Circulation of cholesterol between lysosomes and the plasma membrane. J. Biol. Chem. *273*, 18915–18922.

Lee, W. L., Kim, M. K., Schreiber, A. D., and Grinstein, S. (2005). Role of ubiquitin and proteasomes in phagosome maturation. Mol. Biol. Cell *16*, 2077–2090.

Li, Z., and Sacks, D. B. (2003). Elucidation of the interaction of calmodulin with the IQ motifs of IQGAP1. J. Biol. Chem. *278*, 4347–4352.

Liscum, L. (1990). Pharmacological inhibition of the intracellular transport of low-density lipoprotein-derived cholesterol in Chinese hamster ovary cells. Biochim. Biophys. Acta *1045*, 40–48.

Liscum, L., Ruggiero, R. M., and Faust, J. R. (1989). The intracellular transport of low density lipoprotein-derived cholesterol is defective in Niemann-Pick type C fibroblasts. J. Cell Biol. *108*, 1625–1636.

Malik, Z. A., Denning, G. M., and Kusner, D. J. (2000). Inhibition of Ca(2+) signaling by *Mycobacterium tuberculosis* is associated with reduced phagosome-lysosome fusion and increased survival within human macrophages. J. Exp. Med. *191*, 287–302.

Malik, Z. A., Iyer, S. S., and Kusner, D. J. (2001). Mycobacterium tuberculosis phagosomes exhibit altered calmodulin-dependent signal transduction: contribution to inhibition of phagosome-lysosome fusion and intracellular survival in human macrophages. J. Immunol. *166*, 3392–3401.

Mateer, S. C., McDaniel, A. E., Nicolas, V., Habermacher, G. M., Lin, M. J., Cromer, D. A., King, M. E., and Bloom, G. S. (2002). The mechanism for regulation of the F-actin binding activity of IQGAP1 by calcium/calmodulin. J. Biol. Chem. *277*, 12324–12333.

May, R. C., and Machesky, L. M. (2001). Phagocytosis and the actin cytoskeleton. J. Cell Sci. *114*, 1061–1077.

Mellman, I., and Warren, G. (2000). The road taken: past and future foundations of membrane traffic. Cell *100*, 99–112.

Moller, W., Nemoto, I., Matsuzaki, T., Hofer, T., and Heyder, J. (2000). Magnetic phagosome motion in J774A. 1 macrophages: influence of cytoskeletal drugs. Biophys. J. *79*, 720–730.

Myers, J. T., and Swanson, J. A. (2002). Calcium spikes in activated macrophages during Fcgamma receptor-mediated phagocytosis. J. Leukoc. Biol. *72*, 677–684.

Panchuk-Voloshina, N., Haugland, R. P., Bishop-Stewart, J., Bhalgat, M. K., Millard, P. J., Mao, F., and Leung, W. Y. (1999). Alexa dyes, a series of new fluorescent dyes that yield exceptionally bright, photostable conjugates. J. Histochem. Cytochem. *47*, 1179–1188.

Patton, C., Thompson, S., and Epel, D. (2004). Some precautions in using chelators to buffer metals in biological solutions. Cell. Calcium *35*, 427–431.

Peters, C., and Mayer, A. (1998). Ca2+/calmodulin signals the completion of docking and triggers a late step of vacuole fusion. Nature *396*, 575–580.

Pfeffer, S. R. (1999). Transport-vesicle targeting: tethers before SNAREs. Nat. Cell Biol. *1*, E17–22.

Pitt, A., Mayorga, L. S., Schwartz, A. L., and Stahl, P. D. (1992). Transport of phagosomal components to an endosomal compartment. J. Biol. Chem. *267*, 126–132.

Pryor, P. R., Mullock, B. M., Bright, N. A., Gray, S. R., and Luzio, J. P. (2000). The role of intraorganellar Ca2+ in late endosome-lysosome heterotypic

fusion and in the reformation of lysosomes from hybrid organelles. J. Cell Biol. *149*, 1053–1062.

Scriver, C. R., Beaudet, A. L., Sly, W. S., and Valle, D. (2001). The metabolic and molecular bases of inherited disease. Chapter XVI. Lysosomal disorders. New York: McGraw-Hill.

Sillence, D. J., and Downes, C. P. (1993). Subcellular distribution of agonist-stimulated phosphatidylinositol synthesis in 1321 N1 astrocytoma cells. Biochem. J. *290* (Pt 2), 381–387.

Sionov, R. V., and Gallily, R. (1990). Engulfment and intracellular killing of F9 teratocarcinoma cells by non-activated murine macrophages. Int. Immunol. *2*, 291–301.

Stein, Y., Halperin, G., and Stein, O. (1980). Biological stability of [^{3}H]cholesteryl oleyl ether in cultured fibroblasts and intact rat. FEBS Lett. *111*, 104–106.

Steinman, R. M., Brodie, S. E., and Cohn, Z. A. (1976). Membrane flow during pinocytosis. A stereologic analysis. J. Cell Biol. *68*, 665–687.

Stockinger, W., Castoreno, A. B., Wang, Y., Pagnon, J. C., and Nohturfft, A. (2004). Real-time analysis of endosomal lipid transport by live cell scintillation proximity assay. J. Lipid Res. *45*, 2151–2158.

Storrie, B., and Madden, E. A. (1990). Isolation of subcellular organelles. Methods Enzymol. *182*, 203–225.

Storrie, B., Pool, R. R., Jr., Sachdeva, M., Maurey, K. M., and Oliver, C. (1984). Evidence for both prelysosomal and lysosomal intermediates in endocytic pathways. J. Cell Biol. *98*, 108–115.

Sullivan, P. C., Ferris, A. L., and Storrie, B. (1987). Effects of temperature, pH elevators, and energy production inhibitors on horseradish peroxidase transport through endocytic vesicles. J. Cell. Physiol. *131*, 58–63.

Tapper, H., and Grinstein, S. (1997). Fc receptor-triggered insertion of secretory granules into the plasma membrane of human neutrophils: selective retrieval during phagocytosis. J. Immunol. *159*, 409–418.

Tartakoff, A. M., Gordon, S., and Dalbey, R. E. (1999). Phagocytosis: the host. Amsterdam: Elsevier.

Taunton, J., Rowning, B. A., Coughlin, M. L., Wu, M., Moon, R. T., Mitchison, T. J., and Larabell, C. A. (2000). Actin-dependent propulsion of endosomes and lysosomes by recruitment of N-WASP. J. Cell Biol. *148*, 519–530.

Toyohara, A., and Inaba, K. (1989). Transport of phagosomes in mouse peritoneal macrophages. J. Cell Sci. *94* (Pt 1), 143–153.

Trifaro, J. M., and Vitale, M. L. (1993). Cytoskeleton dynamics during neurotransmitter release. Trends Neurosci. *16*, 466–472.

van Deurs, B., Holm, P. K., Kayser, L., and Sandvig, K. (1995). Delivery to lysosomes in the human carcinoma cell line HEp-2 involves an actin filament-facilitated fusion between mature endosomes and preexisting lysosomes. Eur. J. Cell Biol. *66*, 309–323.

Vergne, I., Chua, J., and Deretic, V. (2003). Tuberculosis toxin blocking phagosome maturation inhibits a novel Ca2+/calmodulin-PI3K hVPS34 cascade. J. Exp. Med. *198*, 653–659.

Vieira, O. V., Botelho, R. J., and Grinstein, S. (2002). Phagosome maturation: aging gracefully. Biochem. J. *366*, 689–704.

Wall, D. A., and Hubbard, A. L. (1985). Receptor-mediated endocytosis of asialoglycoproteins by rat liver hepatocytes: biochemical characterization of the endosomal compartments. J. Cell Biol. *101*, 2104–2112.

Wang, Y., Castoreno, A. B., Stockinger, W., and Nohturfft, A. (2005). Modulation of endosomal cholesteryl ester metabolism by membrane cholesterol. J. Biol. Chem. *280*, 11876–11886.

Wolkoff, A. W., Klausner, R. D., Ashwell, G., and Harford, J. (1984). Intracellular segregation of asialoglycoproteins and their receptor: a prelysosomal event subsequent to dissociation of the ligand-receptor complex. J. Cell Biol. *98*, 375–381.

Worth, R. G., Kim, M. K., Kindzelskii, A. L., Petty, H. R., and Schreiber, A. D. (2003). Signal sequence within Fc gamma RIIA controls calcium wave propagation patterns: apparent role in phagolysosome fusion. Proc. Natl. Acad. Sci. USA *100*, 4533–4538.

Yates, R. M., Hermetter, A., and Russell, D. G. (2005). The kinetics of phagosome maturation as a function of phagosome/lysosome fusion and acquisition of hydrolytic activity. Traffic *6*, 413–420.

Yoshimura, T., Shono, M., Imai, K., and Hong, K. (1995). Kinetic analysis of endocytosis and intracellular fate of liposomes in single macrophages. J. Biochem. *117*, 34–41.

Zimmerli, S., Majeed, M., Gustavsson, M., Stendahl, O., Sanan, D. A., and Ernst, J. D. (1996). Phagosome-lysosome fusion is a calcium-independent event in macrophages. J. Cell Biol. *132*, 49–61.